ROBERT C. BEAL

OCEAN RESEARCH WITH SYNTHETIC APERTURE RADAR

From its inception more than a decade ago, synthetic aperture radar (SAR) oceanography at APL has grown into a substantial interdepartmental effort involving many aspects of science and engineering. This article presents a brief tutorial of aperture synthesis and highlights APL's past, present, and potential future role in SAR oceanography.

INTRODUCTION

Ocean imagery collected with spaceborne synthetic aperture radar (SAR) contains information on surface winds, ocean wavelengths and directions, current fronts and eddies, and, occasionally, coastal bathymetry. Although our present inventory of SAR ocean imagery comes largely from Seasat (a dedicated ocean satellite that performed for only three months in 1978), similar SAR imagery has also been collected from two short Shuttle missions during 1981 and 1984. The unique advantage of SAR for 24-hour, all-weather ocean imaging is now well established for some specific applications; its utility for other applications is likely to increase, especially when SAR is used in conjunction with other information sources and remote sensors.

The concept of aperture synthesis is straightforward in terms of classical diffraction theory, but the practical implementation of SAR generally requires a stable platform, a high bandwidth data link, a substantial memory array, and a rapid processing capability.

APERTURE SYNTHESIS (adapted from Ref. 1)

Azimuth Resolution

According to classical diffraction theory, the angular resolution of any transmitting or receiving system, including SAR, is ultimately limited by the size of its aperture. Expressed simply,

$$\phi = 1/n, \tag{1}$$

where ϕ is the angular resolution and n is the size of the aperture expressed in wavelengths. When the same aperture is used for both the transmitter and the receiver of energy, as it is in SAR, the resulting angular resolution ϕ' is effectively halved ($\phi' = \phi/2$). Figure 1 shows the satellite geometry, typical of Seasat SAR parameters, with a satellite orbiting at an altitude h (or slant range h for near-nadir geometry) of 10^6 meters and containing a SAR that operates at a radar wavelength λ of 0.2 meter. The length of the synthetic aperture, L, is related to the azimuth resolution (the ground resolution in the flight direction of the spacecraft) r_a by

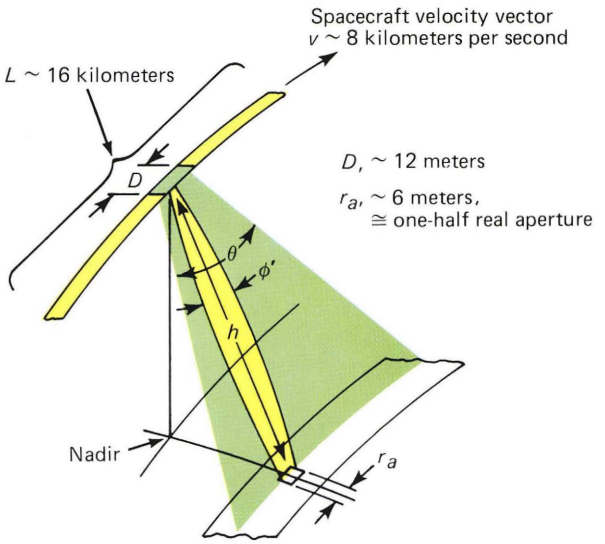

Figure 1—Ultimate resolution of a synthetic aperture.

$$r_a = \phi' h = \frac{\lambda}{2L} h. \tag{2}$$

An azimuth resolution of 25 meters requires a synthetic aperture of 4 kilometers. A satellite traveling at an altitude of 10^6 meters has an orbital velocity of about 8 kilometers per second and therefore requires about 0.5 second to synthesize the required aperture.

Note that the length of the real aperture D on the spacecraft has not explicitly entered into the equations. However, the real aperture must be short enough to allow a particular point on the ground to remain entirely within the real beam $\theta = \lambda/D$ during the aperture synthesis interval, thus leading to the relationship (again illustrated in Fig. 1)

$$L = h \frac{\lambda}{D}. \tag{3}$$

Combining Eqs. 2 and 3 leads to the fundamental lower limit for resolution,

$$r_a = D/2 \,. \qquad (4)$$

Therefore, if a ground resolution of 25 meters is desired, the real aperture can be no longer than 50 meters to maintain a point in the real beam for a sufficiently long time. The resolution limit is independent of range because the time during which a particular point is illuminated increases with range, thus allowing a correspondingly larger synthetic aperture to be formed. The Seasat SAR had a real aperture length of about 12 meters and was therefore theoretically capable of an azimuth resolution of 6 meters. This assumes that the maximum allowable synthetic aperture of 16 kilometers could be constructed, a distance that is covered by the satellite in about 2 seconds.

Although a 6-meter azimuth resolution from Seasat is theoretically possible, the imagery is typically processed to yield only 25 meters. That is, only 4 kilometers of synthetic aperture (0.5 second of data) are simultaneously processed. Any 4 kilometers from the total 16-kilometer length will satisfactorily produce a resolution of 25 meters. Moreover, since the predominant system noise in the SAR is caused by "coherent speckle," which tends to be Rayleigh-distributed in amplitude (i.e., there are wide variations in the reflected signal from a resolution element when the illumination angle is slightly varied), each 4-kilometer segment potentially allows an independent sample of the "average" reflectivity distribution. Therefore, the variance within a scene can be reduced considerably by separately processing and combining four independent 25-meter images.

Thus far the discussion has dealt with only the very basic criteria for obtaining high-azimuth resolution along the velocity vector of the satellite. We have not examined the actual mechanics of collecting and processing the information to reform the image, nor have we expanded our discussion to include the orthogonal (range) dimension. It should be apparent, however, that the synthetic aperture must be constructed with extreme care to realize its full potential. For example, the azimuth resolution suffers if the satellite is perturbed from the perfect trajectory by a significant fraction of its operating wavelength (23 centimeters for Seasat) as it traces out the 16-kilometer aperture. This is analogous to forming an image in a camera with a scratched or distorted lens. Various types of aberrations can occur, all of which lead ultimately to loss of resolution and contrast in the image.

Forming the Image

Having explored some of the fundamental requirements for aperture synthesis, Fig. 2 summarizes schematically the major steps in forming an image in terms of a stationary point-source response. Because an imaging system must be essentially linear, superposition arguments can extend the results to an arbitrary distribution of radar backscatter. A point source (step 1 on the figure), having been illuminated by a coherent radar, emits a series of concentric wavefronts (step 2). The emission occurs only while the point source is within the aperture beam, as was discussed above. The spacecraft cuts through the concentric wavefronts (step 3), and the SAR receiver intercepts an energy flux that varies with position (or time) as the wavefronts are traversed (step 4). This wavefront record is usually referred to as the Doppler (or signal) history, but it can also be considered a hologram, a diffraction pattern, or a one-dimensional zone plate. The essential point is that the wavefront record, which contains a

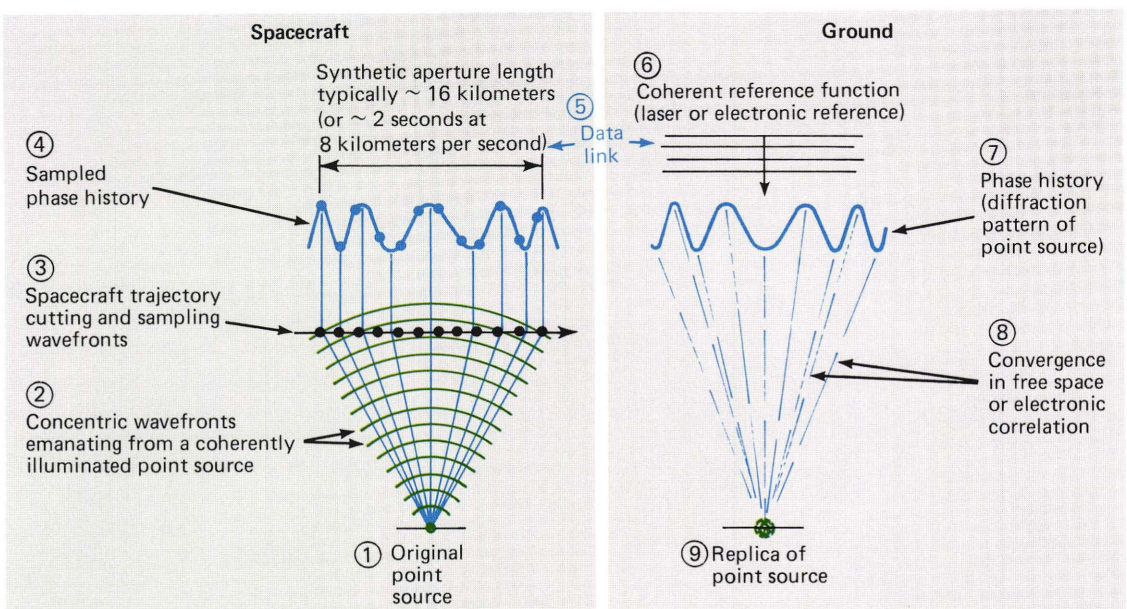

Figure 2—Construction of a synthetic aperture. The replica (9) of the original point source (1) is contaminated by oscillator instability, atmospheric turbulence, data link and film dynamic range, optical aberrations, and electronic truncation.

complete phase and amplitude history of the point source for the entire synthetic aperture interval, contains adequate information to reproduce a diffraction-limited version of the original point source. For Seasat, the wavefront record was transferred from the spacecraft to any of several ground stations through a data link (step 5), where it was recorded on either digital tape or optical film. The signal was normally recorded on tape at the station and was later transferred to film at a central facility. To reproduce the point source from the wavefront record, a coherent reference function (such as a family of plane waves from a laser) (step 6) impinges on the Doppler history (step 7). The Doppler history, which is essentially the diffraction pattern of a point source, causes a lens-free convergence of the plane waves in free space (step 8) and forms a replica of the original point source.

In practice, there are several variations to the simple scheme described in Fig. 2, some of which are helpful, some nuisances, and others irrevocably destructive. A simple lens inserted at step 8 can shorten the convergence distance. On the other hand, the spacecraft trajectory (step 3) is better described by an arc of varying center of curvature than by a straight line. Thus, the diffraction pattern becomes a function of time; this is clearly a nuisance, entailing an adaptive processing strategy. Atmospheric turbulence, reference function instabilities, and lens aberrations are examples of destructive and largely uncorrectable sources of contamination. Much of the effort and expense of spaceborne SAR can be attributed to the need to account precisely for the systemic sources of contamination and to minimize the random sources.

Constructing the Two-Dimensional Image

The extension of SAR image formation to the range (cross-velocity) direction is straightforward, but it places strict timing and synchronization requirements on the design and severely restricts the total range interval (or corresponding ground swath width) that can be accommodated. Range information is possible in a SAR only because the synthetic aperture need not be continuous but may be constructed with samples; that is, the transmitter may be pulsed. It is enough that one pulse be transmitted each time the real aperture moves by half its length. This is called "filling the aperture," and it leads to a maximum time interval τ of $D/2v$ during which range information can be collected. For $D = 12$ meters and $v = 8$ kilometers per second, $\tau = 750$ microseconds. In practice, the aperture is slightly "overfilled" to reduce the possibility of spurious signals that could lower image contrast. The Seasat SAR, for example, typically operated at an interpulse period of 600 microseconds. Moreover, somewhat less than half of that time interval represented signals of sufficient quality to produce good imagery.

Figure 3 shows the synchronization constraints imposed by the Seasat geometry. Transmitter pulses are emitted every 600 microseconds in the cross-track direction, 20 degrees away from nadir. The pulses form concentric expanding rings of energy with a separation of about 200 kilometers ($c\tau = 3 \times 10^8$ meters per second $\times$ 600 $\times$ 10^{-6} seconds $\cong$ 200 kilometers). With the satellite orbiting at an altitude of 800 kilometers, there are four such pulses descending at any time. Since the antenna illuminates only that region around 20 degrees from nadir, no significant backscatter occurs except at a slant range of about 850 kilometers. This is no accident because the round-trip distance of 1700 kilometers must be chosen to allow the return from a particular pulse to occur exactly between two subsequently transmitted pulses. The geometry and pulse interval for the Seasat SAR were chosen to allow the return from a given pulse to occur exactly midway between the eighth and ninth subsequent pulses. As Fig. 3 shows, the middle 250 microseconds

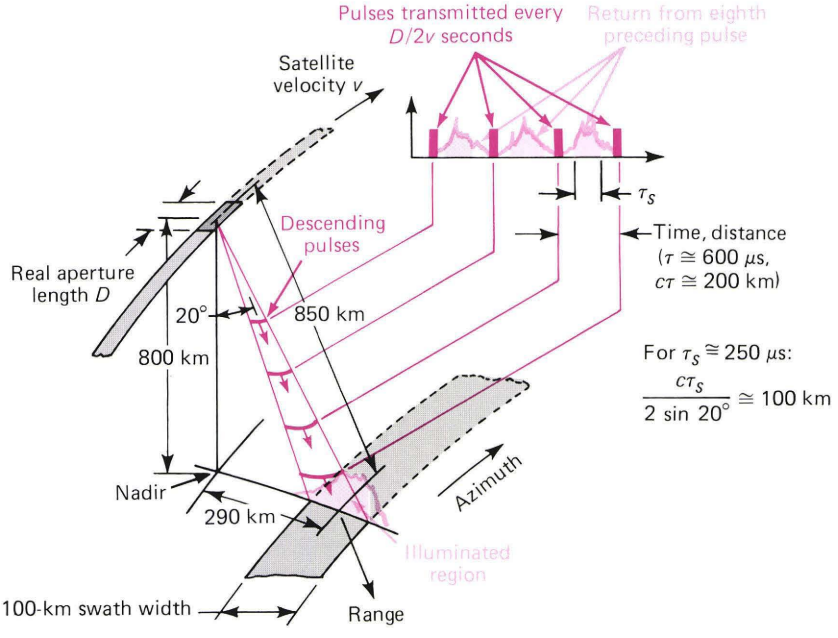

Figure 3—Synchronization constraints in the Seasat SAR.

of return, τ_s, represent a swath width of about 100 kilometers for the Seasat geometry. Large swaths inherently require long real apertures to accommodate adequately all ranges and simultaneously fill the synthetic aperture properly, a serious limitation in spaceborne SAR.

APL's ROLE IN SAR OCEANOGRAPHY

The Pre-Seasat Era

APL's entry into SAR oceanography occurred around 1974, in the form of a conceptual design for the collection of global ocean wave spectra,[2] performed for NASA Headquarters as part of an early systems design of Seasat. Unfortunately, cost-savings measures taken later in the program eliminated the high-speed on-board recorder necessary for the global collection scheme. Merely proposing the concept, however, forced us to understand the important components of the end-to-end SAR system and its associated error sources. As a direct result, we were able to propose and implement an inexpensive analog SAR data link[3] and the associated ground station equipment.[4]

Even in 1974, there was considerable debate over the utility of SAR for ocean imaging; the chief concern was the effect of a moving ocean on image quality. The most pessimistic view held that the SAR, being essentially a Doppler measurement technique, would be completely unable to image a moving field of scatterers. Between 1975 and 1977, there were many forces working to eliminate the SAR from the Seasat instrument package; detractors said it was too expensive, data handling and processing would be impractical, and its scientific value to oceanography was highly speculative and unproven. In short, it was a risky venture.

On the other hand, high-resolution, all-weather radar images from space had an air of the exotic and certainly represented a substantial technical challenge. To NASA's credit, this point of view prevailed, and the SAR, albeit stripped of some of its frills such as on-board recording and digital processing, remained in the plan. Consequently, for 100 days during the late summer and early fall of 1978, Seasat yielded its amazing harvest of ocean images (see Fig. 4 for some examples), showing a richness and variety of spatial patterns completely unanticipated by even its most optimistic supporters. The interpretation and application of these geophysically induced patterns have been and remain a central theme of SAR ocean research at APL.

The Seasat Era

In the early summer of 1978, using discretionary funds from the Director's Office and surplus cameras from the Navy, APL constructed an imaging system to investigate the dynamics of small 30-centimeter waves (those responsible for the spatial patterns on Seasat SAR L-band imagery) in an actual field environment off Hatteras, directly within the anticipated SAR swaths. Ironically, the analysis of the effort was ultimately inconclusive, but it did provide sufficient rationale for the mission planners to excite the severely power-rationed SAR nearly every time it passed over the east coast. The unique U.S. east coast data set later formed the basis for an international symposium on SAR Oceanography[5] held at APL in early 1980. Within the data set was a particularly interesting pass (pass 1339, September 28) that, because of the associated meteorology and simultaneous measurements available, has since provided significant insight into the SAR's capabilities.[6-10] Irvine and Gerling report on various aspects of the pass in articles elsewhere in this issue.

Data processing for Seasat was initially underfunded in this country; the first high-quality SAR digital processor was funded by the Canadian government and produced in 1979 by MacDonald Dettwiler and Associates in Vancouver. In the United States, the Jet Propulsion Laboratory produced the first digital images in 1980. Since then, the processing capability has expanded to organizations in Britain, Norway, Germany, and Japan. In this country, in the past two years, both the Naval Research Laboratory and APL (see McDonough et al. elsewhere in this issue) have implemented high-quality flexible digital processors.

The Shuttle Era

In the aftermath of Seasat, NASA's program to exploit SAR science and applications has become multidisciplinary, expanding from oceans to include geology, hydrology, vegetation, and, with the next Shuttle experiment, polar ice mapping. Faced with a combination of budget austerity and conflicting instrument desires from the various disciplines, NASA chose to exploit the Shuttle program to achieve a multiyear series of flexible SAR experiments of gradually increasing complexity. Since Seasat, the Shuttle Imaging Radar (SIR) series, managed by the Jet Propulsion Laboratory, has become this country's major means for exploring scientific applications of SAR. Although typically of only a few days' duration, enough data can be accumulated to make significant progress in most disciplines. The major disadvantage for oceanographic experiments has been logistical: unexpected launch delays increase the risk of scheduling comprehensive field experiments in the open ocean and polar regions.

The first Shuttle Imaging Radar (SIR-A) flew in November 1981. The instrument was identical to that of Seasat (L band), but an off-nadir angle of 45 degrees was chosen to favor geological imaging rather than ocean imaging. The emphasis on geology was partly fueled by the renewed interest in a Venus Radar Mapper that is now scheduled for a 1987 launch. As a result and also because the SIR-A system was designed around a lower quality optical processor, there was little interest in the 1981 mission for oceanography. However, SIR-A did manage to capture several distinct groups of internal solitons in the Sulu Sea (see Apel et al. elsewhere in this issue) in spite of its low inclination (28 degrees) and limited data set.

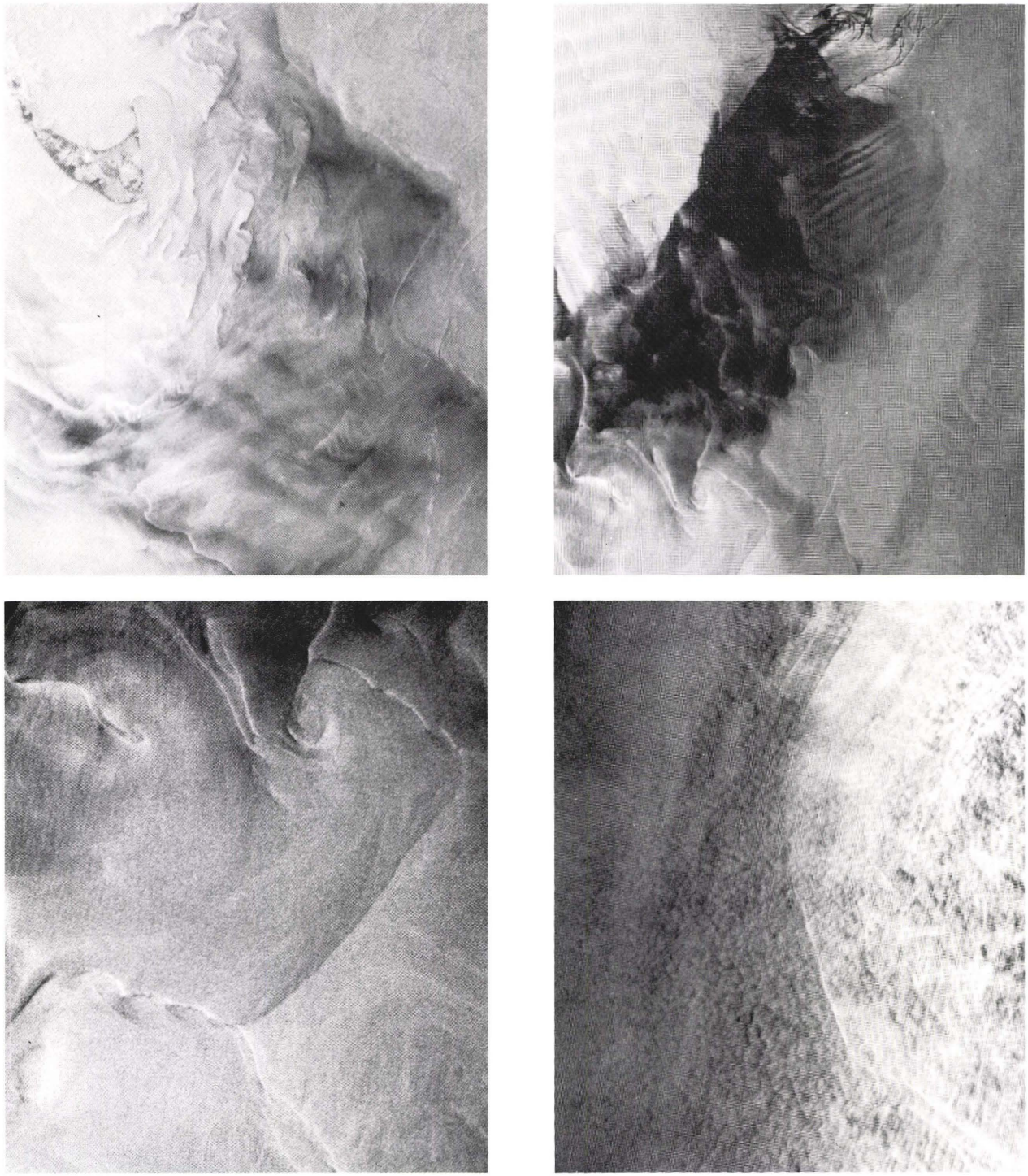

Figure 4—Surface expressions of various geophysical processes revealed in Seasat SAR imagery. Top left, a 100-kilometer-long SAR image of Nantucket Shoals provides a dramatic example of bathymetric expressions occasionally evident over large areas. Most of the region included in this image is less than 40 meters deep, a good fraction is less than 20 meters deep, and portions are less than 2 meters deep. The island of Nantucket is at the upper left. Top right, a 100-kilometer-long SAR image located just outside the entrance of the Chesapeake Bay. Surface wind is essentially calm ($U_{10} \leq 1$ meter per second) in the center (dark) region and gradually increases toward the edges. Surface roughness patterns on this scale reflect not only surface wind patterns but spatial changes in air-sea temperature differences, which directly affect the surface drag coefficient. Bottom left, a 40-kilometer-long SAR image located just north of the Gulf Stream as it veers eastward from Hatteras. Mesoscale water mass boundaries and eddies have strong expressions on the radar imagery. A 200-meter wavelength swell system of significant wave height (1 meter) is traveling from the lower right toward the upper left. Bottom right, a 100-kilometer-long SAR image passing over the western half of a large warm water ring less than a month before it begins to merge again with the Gulf Stream. Warm ring boundaries, perhaps representing current shear zones, are particularly evident in the radar imagery. The brighter radar signature inside the ring may be at least partially due to the increased surface drag at warmer temperatures.

The most recent of the Shuttle SAR experiments (SIR-B) occurred in October 1984 and had the additional attributes of a variable incidence angle (15 to 60 degrees), higher inclination (57 degrees), and high-quality calibrated digital processing. The SIR-B experiments were truly international in scope, with more than 40 separate investigations centered on every continent except Antarctica. There were a number of important ocean experiments, two of the more comprehensive of which were conceived and executed by APL. Off the New York Bight, the SAR Signature Experiment[11] (see also Gasparovic et al. and Thompson elsewhere in this issue) was designed to validate and refine SAR imaging models of internal waves. The Extreme Waves Experiment in the southern hemisphere was an attempt to explore the ability of SAR ocean wave imaging to update global forecast models[12,13] (see Monaldo elsewhere in this issue). Analysis of the SIR-B data set will continue at least through 1986.

Because there were some serious problems with the SIR-B experiment, only about 10 percent of the initial experiment plans were satisfied. (The two APL experiments fared better than most.) As a result, a reflight of the SIR-B experiment (SIR-B′) is now scheduled for March 1987. Priority will be given to those experiments least satisfied in the original SIR-B plan; however, the reflight orbit will be nearly polar, so there will also be an unprecedented opportunity for polar ice mapping.

The next major expansion of the Shuttle SAR capabilities will come in 1989 and 1990, with two SIR-C flights, both of which will feature multifrequency (L, C, and X bands), multipolarization (including cross polarization), and variable incidence angle.[14] A flexible format will allow various combinations of interleaving modes to accommodate individual tailored experiments. As in SIR-B, the SIR-C experiment plan will result from a competitive proposal review process that is scheduled to begin in early 1986. In addition, there may be separate agreements between NASA and the Office of Naval Research to collect additional data in support of various field experiments. For example, for SIR-B′, the Navy is requesting data in a marginal ice zone, in a region of probable high seas, and in a region of strong frontal activity.

TOWARD FREE FLYERS

Free-flying SARs, with lifetimes of years rather than days, are clearly necessary for solving any operational problem, and there are several plans to implement such systems beginning around the end of the decade. In the early to mid-1990s, the NASA Shuttle series is expected to evolve into a prototype for the Earth Observing Station, which is currently envisioned as a multiplatform, multisensor concept for monitoring long-term (10-year) environmental changes related to global habitability (see McGoldrick, this issue). In this context, SAR may have an important role to play as a complement to precision altimetry for understanding global circulation and coastal mixing processes. The role of SAR in the ocean circulation problem is not yet clear, since the appropriate controlled experiments have yet to be conducted. However, the unique ability of SAR to reveal mesocale and smaller ocean features has been well documented in the Seasat data set for surface winds below about 7 meters per second.

The first quasi-operational free-flying SAR, ERS-1, will be launched by the European Space Agency around 1990 and will have a Seasat-like orbit and instrument complement. With simultaneous operation from an altimeter and a scatterometer, and interleaving SAR imagery, it is directed specifically toward ocean and atmospheric research. The European Space Agency is encouraging foreign investigations and is planning to solicit proposals in 1986.

Beyond ERS-1, the Canadians are planning a wide-swath SAR, Radarsat, sometime after 1990, chiefly for ice reconnaissance in their polar regions. Also, possibly in the mid-1990s, the U.S. Navy is considering a SAR for the second version of the U.S Navy Remote Ocean Sensing System (NROSS-2). Such a SAR on a high-altitude platform would be most useful for ice reconnaissance and perhaps current front and eddy mapping. However, for the global wave forecasting problem, evidence from SIR-B analysis is accumulating in favor of a low-altitude, dedicated satellite.[12,13,15] Efforts are currently under way at APL to produce a conceptual design for such a system that would feature synthetic aperture resolution from a "GEOSAT-class" satellite.

REFERENCES

1. R. C. Beal, "The Seasat Synthetic Aperture Radar Experiment," *APL Tech. Dig.* **16**, 2-11 (1977).
2. *Seasat-A Definition Phase Baseline Mission Report,* JHU/APL SDO 3831, pp. 2-27—2-77 (1974).
3. E. F. Prozeller, R. J. Heins, and W. C. Trimble, "The Seasat Synthetic Aperture Radar Data Link," *APL Tech. Dig.* **16**, 12-19 (1977).
4. C. May, "Ground Station Equipment for the Seasat SAR," *APL Tech. Dig.* **16**, 20-26 (1977).
5. R. C. Beal, P. S. DeLeonibus, and I. Katz, eds., *Spaceborne Synthetic Aperture Radar for Oceanography,* The Johns Hopkins Oceanographic Studies No. 7, The Johns Hopkins University Press, Baltimore and London (1981).
6. R. C. Beal, F. M. Monaldo, and D. G. Tilley, "Large- and Small-Scale Spatial Evolution of Digitally Processed Ocean Wave Spectra from the Seasat Synthetic Aperture Radar," *J. Geophys. Res.* **88**, 1761-1778 (1983).
7. F. M. Monaldo, "Improvement in the Estimate of Dominant Wavenumber and Direction from Spaceborne SAR Image Spectra When Corrected for Ocean Surface Movement," *IEEE Trans. Geosci. Remote Sensing* **GE-22**, 603-604 (1984).
8. D. G. Tilley, "The Use of Speckle for Determining the Response Characteristics of Doppler Imaging Radars," Society of Photo-Optical Instrumentation Engineers 27th Annual Symp., San Diego (Aug 19-25, 1985).
9. R. C. Beal, T. W. Gerling, D. E. Irvine, F. M. Monaldo, and D. G. Tilley, "Spatial Variations of Ocean Wave Directional Spectra from the Seasat Synthetic Aperture Radar," *J. Geophys. Res.* (in press, 1985).
10. T. W. Gerling, "Structure of the Surface Wind Field from the Seasat SAR," *J. Geophys. Res.* (in press, 1985).
11. R. F. Gasparovic, J. R. Apel, D. R. Thompson, and J. S. Tochko, "A Comparison of SIR-B Radar Data with Internal Wave Measurements via a SAR Imaging Theory," *Science* (in press, 1985).
12. R. C. Beal, "Predicting Dangerous Ocean Waves with Spaceborne Synthetic Aperture Radar," *Johns Hopkins APL Tech. Dig.* **5**, 346-359 (1984).
13. R. C. Beal, F. M. Monaldo, D. G. Tilley, D. E. Irvine, E. J. Walsh, F. C. Jackson, D. W. Hancock III, D. E. Hines, R. N. Swift, F. I. Gonzalez, D. R. Lyzenga, and L. F. Zambresky, "A Comparison of SIR-B Directional Ocean Wave Spectra with Aircraft Scanning Radar Spectra and Global Spectral Ocean Wave Model Predictions," *Science* (in press, 1985).
14. *Shuttle Imaging Radar-C Science Plan,* JPL Pub. 85-65 (1985).
15. R. C. Beal and R. Jordan, "Global Wave Spectra from SAR: System Design Considerations," in *Oceans '84 Conf. Record,* pp. 129-133 (Sep 10-12, 1984).

THE AUTHOR

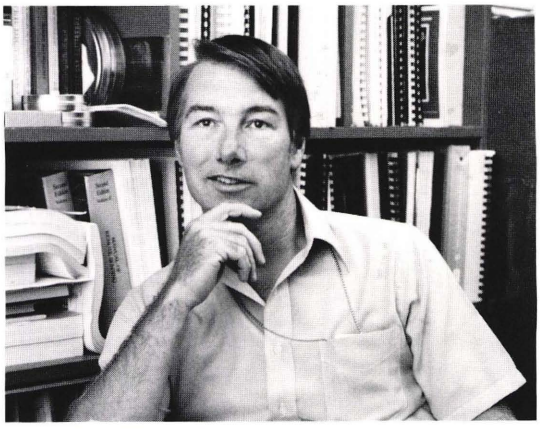

ROBERT C. BEAL is currently assistant group supervisor of APL's Space Geophysics Group. He was born in Boston in 1940 and received a B.S.E.E. from MIT in 1961 and an M.S. in physics from the University of Maryland in 1968. He has been involved in various aspects of spaceborne imaging systems for 20 years and in their ocean applications for 10 years. Mr. Beal has conducted ocean wave experiments with both Seasat and SIR-B and recently has participated in SAR planning activities with both NASA and the Office of Naval Research. In 1984, he organized a major ocean wave experiment off the coast of Chile with SIR-B and is anticipating a follow-on experiment in the Labrador Sea in 1987 with SIR-B′.